J. Plasma Physics (2001), *vol.* 65, *part* 4, *pp.* 319–329. © 2001 Cambridge University Press
DOI: 10.1017/S0022377801001118 Printed in the United Kingdom

Instability of higher-harmonic electrostatic dust cyclotron waves

G. SORASIO and M. ROSENBERG

Department of Electrical and Computer Engineering, University of California, San Diego, La Jolla, CA 92093, USA

(Received 11 November 2000)

Abstract. Conditions for exciting higher-harmonic electrostatic dust cyclotron waves in a collisional dusty plasma are investigated. Linear kinetic theory is used, and the effects of neutral–charged particle collisions are taken into account. In a plasma with negatively charged dust, electrostatic dust cyclotron waves can be driven unstable by ions drifting along the magnetic field. It is found that, under certain conditions, the critical ion drift for the excitation of higher-harmonic electrostatic dust cyclotron waves (i.e., $\omega \sim m\Omega_d$, where $m \geqslant 2$ and Ω_d is the dust cyclotron frequency) can be comparable to the critical drift for the excitation of the fundamental cyclotron harmonic (i.e., $\omega \sim \Omega_d$). Stability conditions are investigated for ranges of parameters that may be relevant to laboratory dusty plasmas.

1. Introduction

In an electron–ion plasma, electrostatic ion cyclotron (EIC) waves can be driven unstable by electrons drifting along the magnetic field. The critical electron drift for exciting EIC waves, with frequency of the order of the ion cyclotron frequency, $\omega \sim \Omega_i$, is one of the lowest among current-driven instabilities (Rasmussen 1988). Excitation of higher-harmonic ion cyclotron waves, $\omega \sim m\Omega_i$, where $m \geqslant 2$, generally requires larger critical drifts, as indicated by the analytical results of Kindel and Kennel (1971) and the numerical simulations of Okuda et al. (1981).

Recently, the electrostatic dust cyclotron instability (EDCI) was investigated in a collisional dusty plasma (D'Angelo 1998; Rosenberg and Chow 1999), and in the collisionless regime (Das et al. 1998; Shukla and Rahman 1998). The EDCI is the analog of the EIC instability (EICI) in the very low dust-cyclotron frequency regime, $\omega \sim \Omega_d$, where $\Omega_d = eZ_dB/m_dc$. The charge-to-mass ratio of dust grains, $|eZ_d/m_d|$, is generally orders of magnitude smaller than that of the ions. In this low-frequency regime, damping due to dust–neutral collisions can be important. In a plasma with negatively charged dust, EDC waves can be driven unstable by ions drifting along **B** (D'Angelo 1998; Rosenberg and Chow 1999). While the latter works considered the conditions for instability of the fundamental harmonic, $\omega \sim \Omega_d$, in this paper, we investigate conditions for exciting the higher harmonics, $\omega \sim m\Omega_d$, where $m \geqslant 2$. For the EDCI, there is a large wavelength regime in which collisionless damping effects can be small, as compared with the EICI, so that critical drifts for exciting higher harmonics can be comparable to that for exciting the fundamental, under certain conditions.

We use a kinetic analysis and include the effects of charged-particle collisions

https://doi.org/10.1017/S0022377801001118 Published online by Cambridge University Press

with neutrals. The analysis is given in Sec. 2. Analytical and numerical results are given in Secs 3 and 4 respectively. Section 5 gives a discussion of a possible laboratory plasma application.

2. Analysis

The analysis extends that of Rosenberg and Chow (1999), who considered the instability of EDC waves with $\omega \sim \Omega_d$, to investigate the excitation of higher-harmonic EDC waves. We consider a weakly ionized plasma composed of negatively charged dust, electrons and singly charged positive ions, in a neutral background. The dust has uniform radius a (and thus uniform charge state Z_d and mass m_d). The condition of charge neutrality is

$$n_e + Z_d n_d = n_i. \tag{1}$$

The relative amount of negative charge density carried by the dust can be characterized by the parameter $\delta = n_i/n_e$ (as δ increases, the negative charged density increases).

There is a magnetic field $\mathbf{B}$ in the z direction, with a constant current along $\mathbf{B}$ (driven, for example, by an electric field $\mathbf{E}_0 \parallel \mathbf{B}$), so the electrons and ions drift in opposite directions relative to the dust in the frame in which the dust is stationary. Using drifting Maxwellians for the electron and ion velocity distributions, and a Maxwellian for the dust velocity distribution, and considering the frequency regime $\omega \ll \Omega_i$, the dispersion relation for electrostatic waves is (Rosenberg and Chow 1999):

$$D(\omega, k) = 1 + \sum_\alpha \chi_\alpha = 0, \tag{2}$$

where

$$\chi_e = \frac{k_{De}^2}{k^2}\left[1 + \zeta_e \Gamma_0(\mu_e) Z(\zeta_e)\right]\left[1 + \frac{i\nu_e}{\sqrt{2}k_z v_e}\Gamma_0(\mu_e) Z(\zeta_e)\right]^{-1}, \tag{3}$$

$$\chi_i = \frac{k_{Di}^2}{k^2}\left[1 + \zeta_i \Gamma_0(\mu_i) Z(\zeta_i)\right]\left[1 + \frac{i\nu_i}{\sqrt{2}k_z v_i}\Gamma_0(\mu_i) Z(\zeta_i)\right]^{-1}, \tag{4}$$

$$\chi_d = \frac{k_{Dd}^2}{k^2}\left[1 + \frac{\omega + i\nu_d}{\sqrt{2}k_z v_d}\sum_{n=-\infty}^{\infty}\Gamma_n(\mu_d) Z(\zeta_d)\right]\left[1 + \frac{i\nu_d}{\sqrt{2}k_z v_d}\sum_{n=-\infty}^{\infty}\Gamma_n(\mu_d) Z(\zeta_d)\right]^{-1}, \tag{5}$$

and

$$\zeta_e = \frac{\omega + k_z u_{0e} + i\nu_e}{\sqrt{2}k_z v_e}, \tag{6}$$

$$\zeta_i = \frac{\omega - k_z u_{0i} + i\nu_i}{\sqrt{2}k_z v_i}, \tag{7}$$

$$\zeta_d = \frac{\omega - n\Omega_d + i\nu_d}{\sqrt{2}k_z v_d}. \tag{8}$$

Here, $\mu_\alpha = k_\perp^2 \rho_\alpha^2$, with ρ_α being the gyroradius of each species, and $\alpha = e, i$, and d denoting ions, electrons and dust, respectively. In addition, $\Gamma_n(z) = I_n(z)e^{-z}$ and I_n is the modified Bessel function of order n, u_{0e} and u_{0i} are the electron and ion drift speeds, $k_{D\alpha} = \sqrt{4\pi Z_\alpha^2 e^2/T_\alpha}$ is the Debye wavenumber, ν_α is the

https://doi.org/10.1017/S0022377801001118 Published online by Cambridge University Press

collision frequency of each charged particle species with neutrals, and Z is the plasma dispersion function (Fried and Conte 1961). For weakly damped or growing waves we can obtain the real, ω_r, and imaginary, γ ($|\gamma| \ll \omega_r$), parts of the frequency using (see e.g. Krall and Trivelpiece, 1973)

$$D_r(\omega_r, k) = 0, \tag{9}$$

$$\gamma = -\frac{D_i(\omega_r, k)}{\left.\dfrac{\partial D_r(\omega_r, k)}{\partial \omega}\right|_{\omega=\omega_r}}, \tag{10}$$

where D_r and D_i are the real and imaginary parts of D.

3. Analytical results

3.1. Weakly collisional case

First we consider the weakly collisional regime, in which both the ion and electron mean free paths, v_i/ν_i and v_e/ν_e respectively, are larger than the wavelength component along $\mathbf{B}$ ($\sim 1/k_z$). Considering also the case where electron and ion Landau damping is small, so that $\omega/k_z \ll v_i, v_e$, and $u_{0i}/v_i \ll 1$, $u_{0e}/v_e \ll 1$, we have that $\zeta_e \ll 1$ and $\zeta_i \ll 1$.

In the limit of small Larmor radii, where $\mu_e \ll 1$, $\mu_i \ll 1$, the electron and ion susceptibilities are then

$$\chi_e \approx \frac{k_{De}^2}{k^2}\left[1 + i\sqrt{\frac{\pi}{2}}\frac{\bar{\omega}_e}{k_z v_e}\left(1 + \sqrt{\frac{\pi}{2}}\frac{\nu_e}{k_z v_e}\right)\right], \tag{11}$$

$$\chi_i \approx \frac{k_{Di}^2}{k^2}\left[1 + i\sqrt{\frac{\pi}{2}}\frac{\bar{\omega}_i}{k_z v_i}\left(1 + \sqrt{\frac{\pi}{2}}\frac{\nu_i}{k_z v_i}\right)\right], \tag{12}$$

where

$$\left.\begin{aligned}\bar{\omega}_e &= \omega + k_z u_{0e},\\ \bar{\omega}_i &= \omega - k_z u_{0i}.\end{aligned}\right\} \tag{13}$$

For the dust, we consider the non-resonant regime, with $\zeta_d \gg 1$. Dust cyclotron damping for the nth harmonic would be negligible when $(\omega - n\Omega_d) \gg k_z v_d$, and we consider this case in the following. Assuming that collisional damping is small, with $\nu_d \ll (\omega - n\Omega_d)$, we have

$$\chi_d \approx \frac{k_{Dd}^2}{k^2}\left\{1 - \sum_n \frac{\omega\Gamma_n(\mu_d)}{\omega - n\Omega_d}\left(1 - \frac{i\nu_d}{\omega - n\Omega_d}\right)\left[1 - \sum_n \frac{i\nu_d\Gamma_n(\mu_d)}{\omega - n\Omega_d}\right]^{-1}\right\}. \tag{14}$$

We assume $\omega = \omega_r + i\gamma$ ($|\gamma| \ll \omega_r$), and write $\omega_r = m\Omega_d(1 + \Delta_m)$, for the mth EDC harmonic. Neglecting all terms of second order in ν_d/Ω_d, using $\omega = m\Omega_d(1 + \Delta_m)$ for the mth harmonic, and $\omega \approx m\Omega_d$ for all the other terms of the summation, we obtain the real part of the dust susceptibility for the mth harmonic mode:

$$\chi_{d,m}^R \approx \frac{k_{Dd}^2}{k^2}\left\{1 - \frac{\Gamma_m(\mu_d)(1 + \Delta_m)}{\Delta_m} - \sum_{n\neq m}\frac{m\Gamma_n(\mu_d)}{m - n}\right\}. \tag{15}$$

For the imaginary part of χ_d, in order to obtain an analytical expression, we make the following approximations: we neglect terms involving the product of two Γ_n functions, and we assume that roughly $(1 + \Delta_m)\Gamma_m/m\Delta_m^2 > \sum_{n\neq m}[m\Gamma_n/(m-n)^2]$

https://doi.org/10.1017/S0022377801001118 Published online by Cambridge University Press

(we note that this appears a good approximation for higher m, for example $m \geqslant 3$ for the numerical case considered in Sec. 4). We then obtain for the imaginary part of χ_d for the mth harmonic

$$\chi^I_{d,m} \approx \frac{k^2_{Dd}}{k^2}\left\{\frac{\nu_d}{\Omega_d}\frac{\Gamma_m(\mu_d)(1+\Delta_m)}{\Delta^2_m m}\right\}. \tag{16}$$

Using these expressions, we can solve (2) for the real and imaginary parts of the frequency, for the mth harmonic. The real part of the frequency is $\omega_r = (1+\Delta_m)m\Omega_d$, where

$$\Delta_m \approx \frac{\Gamma_m(\mu_d)}{[1-G(\mu_d)] + \dfrac{T_d}{T_e}\dfrac{1}{Z_d(\delta-1)}\left(1+k^2\lambda^2_{De}+\delta\dfrac{T_e}{T_i}\right)}, \tag{17}$$

where

$$G(\mu_d) = \Gamma_m(\mu_d) + \sum_{n\neq m}\frac{m\Gamma_n(\mu_d)}{m-n}.$$

The imaginary part of the frequency is

$$\gamma_m \approx -\frac{T_d}{T_e}\sqrt{\frac{\pi}{2}}\frac{1}{Z_d(\delta-1)}\frac{m\Omega_d\Delta^2_m}{\Gamma_m(\mu_d)} \times\left[\frac{\bar{\omega}_e}{k_z v_e}\left(1+\sqrt{\frac{\pi}{2}}\frac{\nu_e}{k_z v_e}\right)+\frac{T_e}{T_i}\delta\frac{\bar{\omega}_i}{k_z v_i}\left(1+\sqrt{\frac{\pi}{2}}\frac{\nu_i}{k_z v_i}\right)\right]-\nu_d(1+\Delta_m). \tag{18}$$

The critical drift can be obtained from (18) by setting $\gamma_m = 0$:

$$\frac{u_{0i}}{v_i} \approx \frac{\omega}{k_z v_i}+\frac{1}{\delta}\frac{u_{0e}}{v_e}\frac{T_i}{T_e}+\sqrt{\frac{2}{\pi}}\frac{\nu_d}{m\Omega_d}\frac{T_i}{T_d}\frac{\Gamma_m(\mu_d)(1+\Delta_m)}{\Delta^2_m}\frac{Z_d(\delta-1)}{\delta}. \tag{19}$$

The k-regimes in which both dust cyclotron damping and ion Landau damping are small are given by

$$\frac{v_i}{v_d}\frac{1}{m(1+\Delta_m)} \gg \frac{k_\perp}{k_z}\frac{1}{k_\perp\rho_d} \gg \frac{1}{m\Delta_m}. \tag{20}$$

Now, $m\Delta_m \approx \frac{1}{2}$ for almost all the harmonics, while the ratio $v_i/v_d \propto (m_d/m_i)^{1/2}$, which can be extremely large (for example, $m_d/m_i \sim 10^9$ for a grain of radius $a \sim 0.1\,\mu$m in a hydrogen plasma). Thus, for the first few harmonics, there can be a relatively large window where both dust cyclotron damping and ion Landau damping are small. As m increases, the window becomes smaller, and, since typically $k_\perp\rho_d$ increases as m increases, dust cyclotron damping becomes more significant for larger m. The analogue of (20) for the electron–ion plasma involves the ratio v_e/v_i (instead of v_i/v_d). For that case, the window in which both ion cyclotron damping and electron Landau damping are small is considerably smaller than in (20). In order to have growth, the value of $k_\perp\rho_i$ has to be large, and, in fact, the mth harmonic of the ion cyclotron waves satisfies $\omega \sim m\Omega_i$ and $k_\perp\rho_i \sim m$ (see Okuda et al. 1981). In a dusty plasma, the values of $k_\perp\rho_d$ do not have to be large and for the first few harmonics, for our set of parameters, they can be less than unity. The approximation $G(\mu) \approx 1$ when $\mu \leqslant m^2$, used by Kindel and Kennel (1971) for the EICI, has to be replaced with a numerical result for the EDCI.

https://doi.org/10.1017/S0022377801001118 Published online by Cambridge University Press

3.2. Strongly collisional case

We consider now the case where the electron and ion mean free paths are smaller than the wavelength component along the magnetic field, so that $\nu_i/k_z v_i \gg 1$, $\nu_e/k_z v_e \gg 1$, and

$$\left.\begin{array}{l} \zeta_e \gg 1, \\ \zeta_i \gg 1. \end{array}\right\} \tag{21}$$

In the limit $\mu_e \ll 1/\zeta_e^2 \ll 1$ and $\mu_i \ll 1/\zeta_i^2 \ll 1$, the electron and ion susceptibilities become

$$\chi_e \approx -\frac{k_{De}^2}{k^2}\frac{k_z^2 v_e^2(\bar{\omega}_e + i\nu_e)}{\bar{\omega}_e(\bar{\omega}_e + i\nu_e)^2 - i\nu_e k_z^2 v_e^2}, \tag{22}$$

$$\chi_i \approx -\frac{k_{Di}^2}{k^2}\frac{k_z^2 v_i^2(\bar{\omega}_i + i\nu_i)}{\bar{\omega}_i(\bar{\omega}_i + i\nu_i)^2 - i\nu_i k_z^2 v_i^2}. \tag{23}$$

First we consider the limit $\nu_e \gg \bar{\omega}_e$, $\nu_i \gg \bar{\omega}_i$, and

$$\left.\begin{array}{l} \dfrac{\nu_e\bar{\omega}_e}{k_z^2 v_e^2} \ll 1, \\ \dfrac{\nu_i\bar{\omega}_i}{k_z^2 v_i^2} \ll 1. \end{array}\right\} \tag{24}$$

In this case, (22) and (23) become

$$\chi_e \approx \frac{k_{De}^2}{k^2}\left(1 + \frac{i\nu_e\bar{\omega}_e}{k_z^2 v_e^2}\right), \tag{25}$$

$$\chi_i \approx \frac{k_{Di}^2}{k^2}\left(1 + \frac{i\nu_i\bar{\omega}_i}{k_z^2 v_i^2}\right). \tag{26}$$

The real part of the frequency is given approximatively by (17), and the imaginary part is

$$\gamma_m \approx -\frac{1}{Z_d(\delta - 1)}\frac{T_d}{T_e}\frac{m\Omega_d\Delta_m^2}{\Gamma_m(\mu_d)}\left(\frac{\nu_e\bar{\omega}_e}{k_z^2 v_e^2} + \frac{T_e}{T_i}\delta\frac{\nu_i\bar{\omega}_i}{k_z^2 v_i^2}\right) - \nu_d(1 + \Delta_m). \tag{27}$$

The growth rate is generally larger than in the weakly collisional case by a factor $\nu_i/k_z v_i \gg 1$. The critical drift is approximately

$$\frac{u_{0i}}{v_i} \approx \frac{\omega}{v_i k_z} + \frac{u_{0e}}{v_e}\frac{T_i}{T_e}\frac{1}{\delta}\frac{v_i}{v_e}\frac{\nu_e}{\nu_i} + \frac{\nu_d}{\nu_i}\frac{\delta - 1}{\delta}\frac{T_i}{T_d}Z_d\frac{\Gamma_m(1 + \Delta_m)}{m\Delta_m^2}\frac{v_i k_z}{\Omega_d}. \tag{28}$$

Next we consider the limit $\nu_e \gg \bar{\omega}_e$, $\nu_i \gg \bar{\omega}_i$, and

$$\left.\begin{array}{l} \dfrac{\nu_e\bar{\omega}_e}{k_z^2 v_e^2} \gg 1, \\ \dfrac{\nu_i\bar{\omega}_i}{k_z^2 v_i^2} \gg 1, \end{array}\right\} \tag{29}$$

to obtain the following electron and ion susceptibilities:

$$\chi_e \approx -\frac{k_{De}^2}{k^2}\frac{k_z^2 v_e^2}{\nu_e^2}\left(1 - \frac{i\nu_e}{\bar{\omega}_e}\right), \tag{30}$$

$$\chi_i \approx -\frac{k_{Di}^2}{k^2}\frac{k_z^2 v_i^2}{\nu_i^2}\left(1 - \frac{i\nu_i}{\bar{\omega}_i}\right), \tag{31}$$

https://doi.org/10.1017/S0022377801001118 Published online by Cambridge University Press

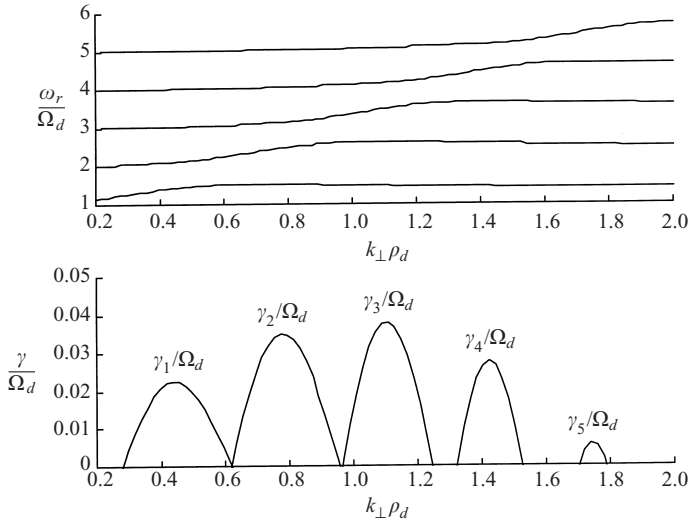


Figure 1. Frequency and growth rate as functions of $k_\perp \rho_d$. The parameters are $u_{0i}/v_i = u_{0e}/v_e = 0.5$, $T_i = T_e = T_d$, $m_i/m_p = 40$, $m_d/m_p = 4 \times 10^6$, $\theta = 82°$, $\omega_{pi}/\Omega_i = 5$, $Z_d = 14$, $\nu_e/\Omega_d = 3414$, $\nu_i/\Omega_d = 12.6$, $\nu_d/\Omega_d = 0.07$, $\delta = 2$.

Using (15) and (16) for the dust susceptibility, we obtain the real part of the frequency for the mth harmonic as $\omega_r = (1 + \Delta_m) m\Omega_d$, where

$$\Delta_m \approx \frac{\Gamma_m(\mu_d)}{[1 - G(\mu_d)] + \dfrac{T_d}{T_e}\dfrac{1}{Z_d(\delta - 1)}\left(k^2\lambda_{De}^2 - \dfrac{k_z^2 v_e^2}{\nu_e^2} - \delta\dfrac{T_e}{T_i}\dfrac{k_z^2 v_i^2}{\nu_i^2}\right)}, \tag{32}$$

and the imaginary part of the frequency is

$$\gamma_m \approx -\frac{1}{Z_d(\delta - 1)}\frac{T_d}{T_e}\frac{m\Omega_d\Delta_m^2}{\Gamma_m(\mu_d)}\left(\frac{k_z^2 v_e^2}{\nu_e \bar{\omega}_e} + \frac{T_e}{T_i}\delta\frac{k_z^2 v_i^2}{\nu_i \bar{\omega}_i}\right) - \nu_d(1 + \Delta_m). \tag{33}$$

4. Numerical results

Figure 1 shows the numerical solutions of (2) for the real part of the frequency and the growth rate in the weakly collisional case using the following parameters: $\theta = 82°$ (where θ is the angle between $\mathbf{k}$ and $\mathbf{B}$ and corresponds to $k_\perp/k_z \approx 7$), $m_i/m_p = 40$ (argon plasma), $m_d/m_p = 4 \times 10^6$ (corresponding to a grain of radius $0.01\,\mu$m and mass density of about $1.6\,\mathrm{g\,cm^{-3}}$), $T_i = T_e = T_d$, $Z_d = 14$ (corresponding to T_e of about $0.5\,$eV and $Z_d \approx 700a(\mu\mathrm{m})|\varphi_s(V)| \approx 14$, with $\varphi_s(V) \sim -4T_e/e$), $u_{0i}/v_i = u_{0e}/v_e = 0.5$, $\omega_{pi}/\Omega_i = 5$ (corresponding to $B \approx 0.8\,$T and $n_i \approx 2.5 \times 10^9\,\mathrm{cm^{-3}}$), and $n_d/n_i = 0.036$, so that $\delta = n_i/n_e \approx 2$. The collisional parameters are $\nu_d/\Omega_d = 0.07$ (corresponding to $n_n \sim 10^{13}\,\mathrm{cm^{-3}}$), $\nu_i/\Omega_d = 12.6$ and $\nu_e/\Omega_d = 3414$. The wavelengths for first few harmonics ($m \leqslant 3$) are in the window (20) where both Landau and dust cyclotron damping are small; the damping for these harmonics is due primarily to dust–neutral collisions, whose effect decreases with increasing m since the ratio $\nu_d/m\Omega_d$ decreases as m increases. For the larger harmonics ($m \geqslant 4, 5$), dust cyclotron damping becomes significant and reduces not only the growth rate but also the region in $k_\perp \rho_d$ where instability occurs. Since for

https://doi.org/10.1017/S0022377801001118 Published online by Cambridge University Press

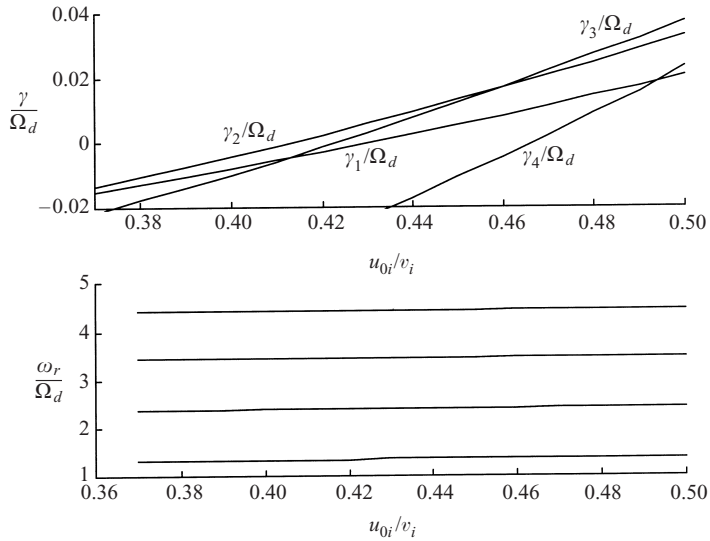


Figure 2. Frequency and growth rate as functions of $u_{0i}/v_i = u_{0e}/v_e$. The parameters are $T_i = T_e = T_d$, $m_i/m_p = 40$, $m_d/m_p = 4\times10^6$, $\theta = 82°$, $\omega_{pi}/\Omega_i = 5$, $Z_d = 14$, $\nu_e/\Omega_d = 3414$, $\nu_i/\Omega_d = 12.6$, $\nu_d/\Omega_d = 0.07$, $\delta = 2$. Here $k_\perp\rho_d = 0.4$ (γ_1/Ω_d), 0.75 (γ_2/Ω_d), 1.1 (γ_3/Ω_d) and 1.4 (γ_4/Ω_d).

the first few harmonics, the most important damping effect is due to dust–neutral collisions, whose effect decreases with increasing m, the second- and third-harmonic modes are driven unstable for a critical drift lower than for the fundamental.

Figure 2 shows the real and imaginary parts of the frequency as functions of the ion drift speed, for various harmonics. The parameters are the same as in Fig. 1, with $u_{0i}/v_i = u_{0e}/v_e$ and fixed $k_\perp/k_z \approx 7$ ($\theta = 82°$), but $k_\perp\rho_d$ is different for each curve. Each curve is for a different harmonic, and is calculated for the value of $k_\perp\rho_d$ that corresponds to the region of maximum growth in Fig. 1 (that is, $k_\perp\rho_d = 0.4$ ($m = 1$), 0.75 ($m = 2$), 1.1 ($m = 3$) and 1.4 ($m = 4$)). It can be seen that the critical drift for exciting the second and third harmonics is lower than that for exciting the first harmonic. Dust cyclotron damping begins to become important for the fourth harmonic, so the critical drift becomes large for that mode.

Figure 3 shows how the critical drift varies as a function of θ, or $k_\perp/k_z$, for the first few harmonics. The parameters are the same as in Fig. 1, so that $u_{0i}/v_i = u_{0e}/v_e$, but each curve represents a different harmonic and is calculated for the value of $k_\perp\rho_d$ that corresponds to the point of maximum growth in Fig. 1 (that is, $k_\perp\rho_d = 0.4$ ($m = 1$), 0.75 ($m = 2$), 1.1 ($m = 3$) and 1.4 ($m = 4$)). It appears that excitation of the second- and third-harmonic modes require lower critical drifts, for this set of parameters. For the first harmonic, as θ increases to 86°, the wavelength regime goes from weakly to strongly collisional, and the destabilizing effect of ion collisions in the strongly collisional regime lowers the critical drift of the fundamental mode compared with the higher harmonics.

Figure 4 illustrates the critical drift versus $\delta = n_i/n_e$ for the first few harmonics. The parameters are the same as in Fig. 1, except that δ and θ are varied. Each curve is calculated for a specific value of $k_\perp\rho_d$ as given above for Figs 2 and 3. The curve in Fig. 4 has been obtained by specifying a value of δ (and of $k_\perp\rho_d$, as explained),

https://doi.org/10.1017/S0022377801001118 Published online by Cambridge University Press

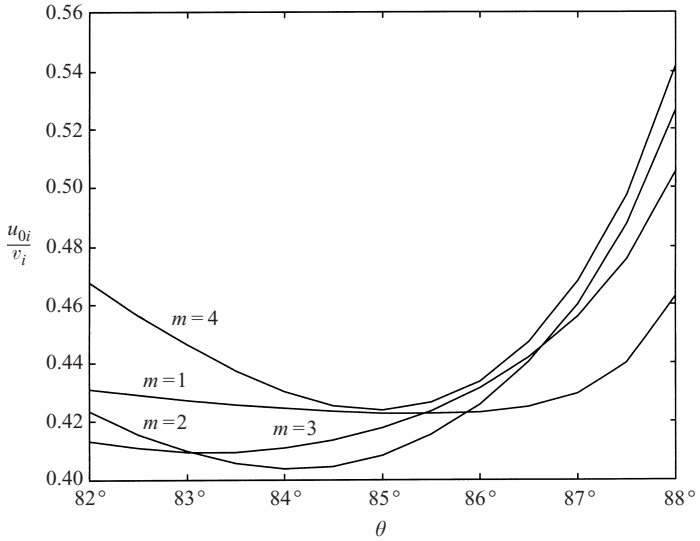


Figure 3. Critical drift as a function of θ. The parameters are $T_i = T_e = T_d$, $m_i/m_p = 40$, $m_d/m_p = 4 \times 10^6$, $\omega_{pi}/\Omega_i = 5$, $Z_d = 14$, $\nu_e/\Omega_d = 3414$, $\nu_i/\Omega_d = 12.6$, $\nu_d/\Omega_d = 0.07$, $\delta = 2$. Here $k_\perp \rho_d = 0.4$ ($m = 1$), 0.75 ($m = 2$), 1.1 ($m = 3$) and 1.4 ($m = 4$).

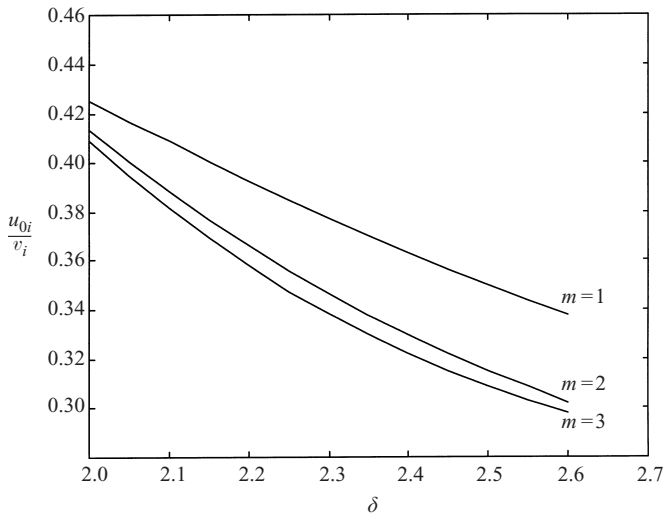


Figure 4. Critical drift as a function of δ. The parameters are $T_i = T_e = T_d$, $m_i/m_p = 40$, $m_d/m_p = 4 \times 10^6$, $\omega_{pi}/\Omega_i = 5$, $Z_d = 14$, $\nu_e/\Omega_d = 3414$, $\nu_i/\Omega_d = 12.6$, $\nu_d/\Omega_d = 0.07$. Here $k_\perp \rho_d = 0.4$ ($m = 1$), 0.75 ($m = 2$) and 1.1 ($m = 3$).

and varying θ in order to obtain the minimum critical drift associated with that δ. The reduction of critical drift as δ increases can be seen from (19) and (28).

5. Discussion

In this paper, we have shown that, under certain conditions, the critical drift for the excitation of higher-harmonic ($m \geqslant 2$) electrostatic dust cyclotron waves may be

https://doi.org/10.1017/S0022377801001118 Published online by Cambridge University Press

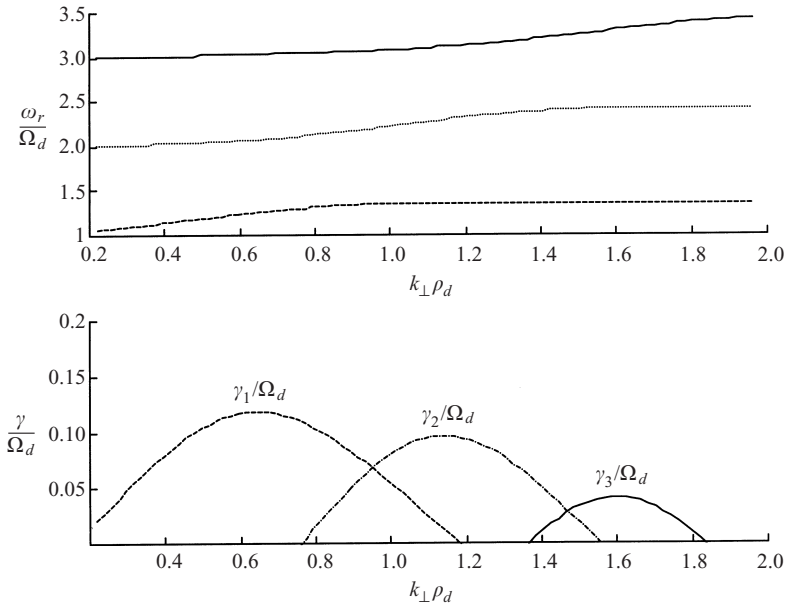


Figure 5. Frequency and growth rate as functions of $k_\perp \rho_d$. The parameters are $T_e/T_i = 6$, $T_e/T_d = 3$, $m_i/m_p = 4$, $m_d/m_p = 10^{11}$, $\theta = 82°$, $\omega_{pi}/\Omega_i = 2.5$, $Z_d = 2000$, $\nu_e/\Omega_d = 2\times10^6$, $\nu_i/\Omega_d = 10^4$, $\nu_d/\Omega_d = 0.045$, $n_d/n_i = 10^{-6}$, $u_{0i}/v_i = (u_{0e}/v_e)T_e/T_i = 0.6$.

comparable to the critical drift for exciting the fundamental mode. The numerical results in Sec. 4 correspond to small grains of size of order 0.01 μm. In order to consider possible laboratory experimental parameters, we consider the case of larger dust of radius $a = 0.3\,\mu$m, since diagnostics may be easier for larger grain sizes. We assume that the dust has mass density $\rho_d = 1.5\,\mathrm{g\,cm^{-3}}$, so that $m_d/m_p \approx 10^{11}$. We assume the following plasma parameters: $T_e = 3\,\mathrm{eV}$, $T_i = 0.5\,\mathrm{eV}$, $n_i = 10^{10}\,\mathrm{cm^{-3}}$ (He plasma), $n_n = 10^{13}\,\mathrm{cm^{-3}}$ (pressure of about 0.3 mTorr) and $B \approx 1\,\mathrm{T}$. In this case, we estimate the dust-charge state $Z_d \approx 700a(\mu\mathrm{m})|\varphi_s(V)| \approx 2000$ (assuming $\varphi_s \sim -10\,\mathrm{V}$), so that $\Omega_d \approx 2\,\mathrm{s^{-1}}$. The dust–neutral collision frequency is

$$\nu_{dn} \approx \pi a^2 n_n v_n \frac{m_n}{m_d} \approx 0.09\,s^{-1} \ll \Omega_d, \tag{34}$$

assuming $v_n \sim 10^5\,\mathrm{cm^{-3}}$. The dust gyroradius can be estimated as $\rho_d \approx v_d/\Omega_d \approx 1.6\,\mathrm{cm}$, assuming $T_d \sim 1\,\mathrm{eV}$. Thus, dust can be magnetized, since $\Omega_d \gg \nu_{dn}$, as long as the radial (i.e. perpendicular to **B**) size of the device is much greater than ρ_d. The other dimensionless parameters are, using the above values $\omega_{pi}/\Omega_i = 2.6$, $\nu_i/\Omega_d = 10^4$, $\nu_e/\Omega_d = 2\times10^6$, $T_e/T_i = 6$, and $T_e/T_d = 3$. We assume the dust density to be sufficiently low that dust acoustic waves (DAW) would be heavily damped, which would occur when the phase speed of the DAW,

$$v_{\mathrm{ph}} \approx \left[Z_d(\delta - 1)\frac{T_e}{m_d}\frac{1}{(1+\delta T_e/T_i)}\right]^{1/2}$$

is of the order of the dust thermal speed $v_d \sim (T_d/m_d)^{1/2}$. Therefore we choose $n_d/n_i = 10^{-6}$.

Assuming that there is an electric field $\mathbf{E}_0$ along **B**, the equilibrium ion and

https://doi.org/10.1017/S0022377801001118 Published online by Cambridge University Press

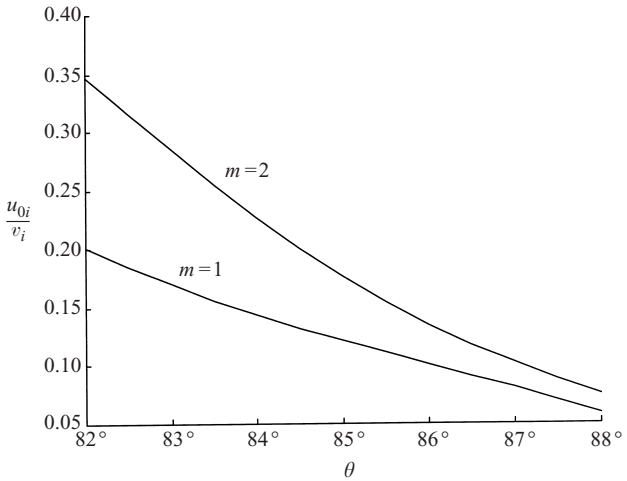


Figure 6. Critical drift as a function of θ. The parameters are $T_e/T_i = 6, T_e/T_d = 3$, $m_i/m_p = 4$, $m_d/m_p = 10^{11}$, $\omega_{pi}/\Omega_i = 2.5$, $Z_d = 2000$, $\nu_e/\Omega_d = 2 \times 10^6, \nu_i/\Omega_d = 10^4$, $\nu_d/\Omega_d = 0.045$, $n_d/n_i = 10^{-6}$. Here $k_\perp \rho_d = 0.65$ ($m = 1$) and 1.1 ($m = 2$) and $u_{0i}/v_i = (u_{0e}/v_e)\, T_e/T_i$.

electron drifts would be given by (see D'Angelo and Merlino 1996)

$$\left.\begin{aligned} \frac{\mathbf{u}_{0i}}{v_i} &\sim \frac{e\mathbf{E}_0}{m_i \nu_i v_i}, \\ \frac{\mathbf{u}_{0e}}{v_e} &\sim -\frac{e\mathbf{E}_0}{m_e \nu_e v_e}. \end{aligned}\right\} \tag{35}$$

Assuming the same cross-sections for He^+–He collisions and for e–He collisions, we have $\nu_i/\nu_e \sim v_i/v_e$, and so $(u_{0i}/v_i) \sim (T_e/T_i)|u_{0e}/v_e|$. Figure 5 shows the real and imaginary parts of the frequency for the parameters given above and for $u_{0i}/v_i = 0.06$ and $\theta = 82°$ ($k_\perp/k_z \approx 7$, which implies the length of the device (i.e. the dimension parallel to **B**) should be much greater than $7/k_\perp$). The wavelengths of the three harmonics are all in the weakly collisional regime. Dust–neutral collisional damping is small in these cases. Ion and electron Landau damping are negligible, but the effect of dust cyclotron damping becomes important for the third harmonic.

Figure 6 shows how the critical drift varies with angle, for the same parameters as in Fig. 5. Each curve represents a different harmonic, and is calculated for the value of $k_\perp \rho_d$ where the corresponding graph in Fig. 5 shows maximum growth (that is, $k_\perp \rho_d = 0.65$ ($m = 1$) and 1.1 ($m = 2$)). The fundamental mode always has the lower critical drift, even if, for larger angles, the critical drifts for excitation of the first two harmonics get closer.

Acknowledgements

This work was supported in part by Grants D0E DE-FG03-97ER54444 and UCSD/LANL 1022. G. Sorasio thanks Kevin Quest for his helpful suggestions. The authors thank Vivian Chow for helpful discussions.

https://doi.org/10.1017/S0022377801001118 Published online by Cambridge University Press

References

D'Angelo, N. 1998 Current driven electrostatic dust cyclotron instability in a collisional plasma. *Planet. Space Sci.* **46**, 1671–1676.

D'Angelo, N. and Merlino, R. L. 1996 Current driven dust acoustic instability in a collisional plasma. *Planet. Space. Sci.* **44**, 1593–1598.

Das, C., Janaki, M. S. and Dasgupta, B. 1998 Dust cyclotron instability in the presence of dust charge fluctuations. *Physica Scripta* **T75**, 216–218.

Fried, B. D. and Conte, S. 1961 *The Plasma Dispersion Function.* Academic Press, New York.

Kindel, J. M. and Kennel, C. F. 1971 Topside current instabilities. *J. Geophys. Res.* **76**, 3055–3078.

Krall, N. A. and Trivelpiece, A. W. 1973 *Principles of Plasma Physics.* McGraw-Hill, New York.

Okuda, H., Cheng, C. Z. and Lee, W. W. 1981 Numerical simulations of electrostatic hydrogen cyclotron instabilities. *Phys. Fluids*, **24**, 1060–1068.

Rasmussen, J. J. 1988 In: *Proceedings of the Workshop on the Current-Driven Electrostatic Ion-Cyclotron Instability* (ed. R. W. Schrittwieser), pp. 42–80. World Scientific, Singapore.

Rosenberg, M. and Chow, V. W. 1999 Collisional effects on the electrostatic dust cyclotron instability. *J. Plasma Phys.* **61**, 51–63.

Shukla, P. K. and Rahman, H. U. 1998 Instability of electrostatic dust-cyclotron waves and associated wake potential. *Planet. Space Sci.* **46**, 541–543.

https://doi.org/10.1017/S0022377801001118 Published online by Cambridge University Press